NAVAL POSTGRADUATE SCHOOL
Monterey, California

THESIS

LOW COST PARACHUTE
GUIDANCE, NAVIGATION, AND CONTROL

by

Scott Henry Dellicker
September 1999

Thesis Advisors:	Isaac. I. Kaminer
	Richard M. Howard

Approved for public release; distribution is unlimited.

REPORT DOCUMENTATION PAGE		*Form Approved* *OMB No. 0704-0188*

Public reporting burden for this collection of information is estimated to average 1 hour per response, including the time for reviewing instruction, searching existing data sources, gathering and maintaining the data needed, and completing and reviewing the collection of information. Send comments regarding this burden estimate or any other aspect of this collection of information, including suggestions for reducing this burden, to Washington headquarters Services, Directorate for Information Operations and Reports, 1215 Jefferson Davis Highway, Suite 1204, Arlington, VA 22202-4302, and to the Office of Management and Budget, Paperwork Reduction Project (0704-0188) Washington DC 20503.

1. AGENCY USE ONLY *(Leave blank)*	2. REPORT DATE March 1998	3. REPORT TYPE AND DATES COVERED Master's Thesis

4. TITLE AND SUBTITLE **LOW COST PARACHUTE NAVIGATION GUIDANCE AND CONTROL**	5. FUNDING NUMBERS
6. AUTHOR(S) Dellicker, Scott Henry	
7. PERFORMING ORGANIZATION NAME(S) AND ADDRESS(ES) Naval Postgraduate School Monterey, CA 93943-5000	8. PERFORMING ORGANIZATION REPORT NUMBER
9. SPONSORING / MONITORING AGENCY NAME(S) AND ADDRESS(ES)	10. SPONSORING / MONITORING AGENCY REPORT NUMBER

11. SUPPLEMENTARY NOTES

The views expressed in this thesis are those of the author and do not reflect the official policy or position of the Department of Defense or the U.S. Government.

12a. DISTRIBUTION / AVAILABILITY STATEMENT Approved for public release; distribution is unlimited.	12b. DISTRIBUTION CODE

13. ABSTRACT *(maximum 200 words)*

The Affordable Guided Airdrop System (AGAS) integrates a low-cost guidance and control system into fielded cargo air delivery systems. This study evaluated the feasibility of this concept and included the design and execution of a flight test program to assess prototype system performance, as well as modeling efforts to develop initial guidance and control techniques, and to evaluate the feasibility of the AGAS concept. The flight test program provided adequate flight dynamic data for the AGAS system. The wind measurement techniques employed through the use of a "calibration" parachute system provided the best possible wind measurement system. Flight test data demonstrated the actuator system can provide glide ratios of 0.4 to 0.5 for a flat circular parachute. A simulation was developed using a point mass model for parachute dynamics, sensor models, and a Bang-Bang type control system. Six hundred simulations demonstrated that the Affordable Guided Airdrop System shows strong potential of providing a low-cost alternative for precision airdrop. Further work is recommended to implement a six degree of freedom dynamic model, assess the dynamic response of the production parachute system, and optimize the control algorithms to minimize fuel usage.

14. SUBJECT TERMS Parachute, Guidance, Navigation, Control, Parameter Estimation			15. NUMBER OF PAGES 73
			16. PRICE CODE

17. SECURITY CLASSIFICATION OF REPORT Unclassified	18. SECURITY CLASSIFICATION OF THIS PAGE Unclassified	19. SECURITY CLASSIFI- CATION OF ABSTRACT Unclassified	20. LIMITATION OF ABSTRACT UL

LOW COST PARACHUTE NAVIGATION, GUIDANCE, AND CONTROL

Scott Henry Dellicker
United States Army
B.S., Rensselaer Polytechnic Institute, 1984

**Submitted in partial fulfillment of the
requirements for the degree of**

MASTER OF SCIENCE IN AERONAUTICAL ENGINEERING

from the

**NAVAL POSTGRADUATE SCHOOL
March 1999**

Author:
_____

Scott Henry Dellicker

Approved by:
_____

Richard M. Howard, Thesis Advisor

_____

Isaac I. Kaminer, Thesis Advisor

_____

**Gerald H. Lindsey ,Chairman
Department of Aeronautics and Astronautics**

ABSTRACT

The Affordable Guided Airdrop System (AGAS) integrates a low-cost guidance and control system into fielded cargo air delivery systems. This study evaluated the feasibility of this concept and included the design and execution of a flight test program to assess prototype system performance, as well as modeling efforts to develop initial guidance and control techniques, and to evaluate the feasibility of the AGAS concept. The flight test program provided adequate flight dynamic data for the AGAS system. The wind measurement techniques employed through the use of a "calibration" parachute system provided the best possible wind measurement system. Flight test data demonstrated the actuator system can provide glide ratios of 0.4 to 0.5 for a flat circular parachute. A simulation was developed using a point mass model for parachute dynamics, sensor models, and a Bang-Bang type control system. Six hundred simulations demonstrated that the Affordable Guided Airdrop System shows strong potential of providing a low-cost alternative for precision airdrop. Further work is recommended to implement a six degree of freedom dynamic model, assess the dynamic response of the production parachute system, and optimize the control algorithms to minimize fuel usage.

TABLE OF CONTENTS

ACKNOWLEDGEMENTS

I.   INTRODUCTION

The United States Air Force Science Advisory board was tasked to develop a forecast of the requirements of the most advanced air and space ideas to project the Air Force into the next century. The study, encompassing all aspects of Air Force operations, assessed a variety of technology developments critical to the Air Force mission. This study culminated in a report titled "New World Vistas, Air and Space Power for the 21st Century."[1] The study identified a critical need to improve the Point-of-Use Delivery; that is, getting the materiel where it needs to be, when it needs to be there. Airdrop is an important aspect of Point-of-Use Delivery. The report indicated that immediate improvements are needed with emphasis provided by the statement: "In the future, the problem of airdrop should be treated as seriously as the problem of bomb drop."

To date, significant emphasis has been placed on the development of large-scale parafoil systems. These systems provide the accuracy required with delivery from high altitude and large offset distances. The drawback is prohibitive cost for each pound of payload delivered. Alternate approaches were required to reduce system cost. Improved Affordable Airdrop Technologies are being evaluated by the team of the United States Army and Air Force, The Boeing Company, and Vertigo, Incorporated. These efforts include the design and development of the Affordable Guided Airdrop System, which incorporates a low-cost guidance, navigation, and control system into fielded cargo air delivery systems. This study focuses on evaluating the feasibility of the AGAS concept and encompassed the design and execution of a flight test program to assess dynamic response of a flat circular parachute, the design of initial guidance and control techniques, and to evaluate the feasibility of the AGAS concept.

II.   SYSTEM DESCRIPTION

A.   AFFORDABLE GUIDED AIRDROP SYSTEM (AGAS)

The Affordable Guided Airdrop System[2] (AGAS) is being evaluated as a low-cost alternative for meeting the military's requirements for precision airdrop. Designed to bridge the gap between expensive high glide parafoil systems and uncontrolled (ballistic) round parachutes, the AGAS concept offers the benefits of high altitude parachute releases but cannot provide the same level of offset from the desired impact point (IP) as high-glide systems. The design goal of the AGAS development is to provide a Guidance, Navigation, and Control (GNC) system that can be placed in-line with existing fielded cargo parachute systems (G-12 and G-11) and standard delivery containers (A-22). The system is required to provide an accuracy of 100 meters, Circular Error Probable (CEP), with a desired goal of 50 meters CEP. No changes to the parachute or cargo system are allowed.

The current design concept includes implementation of commercial Global Positioning System (GPS) receiver and a heading reference as the navigation sensors, a guidance computer to determine and activate the desired control input, and the application of Pneumatic Muscle Actuators (PMAs) to effect the control. The navigation system and guidance computer would be secured to existing container delivery system while the PMAs would be attached to each of four parachute risers and to the container. Figure 1 illustrates the concept. Control is affected by lengthening a single or two adjacent actuators. The parachute deforms creating an unsymmetrical shape, essentially shifting the center of pressure, and providing a drive or slip condition. Upon deployment of the system from the aircraft, the guidance computer would steer the system to a pre-

planned trajectory. This concept relies on the ability of sufficient drive to be produced to overcome errors in wind estimation and the point of release of the system from the aircraft.
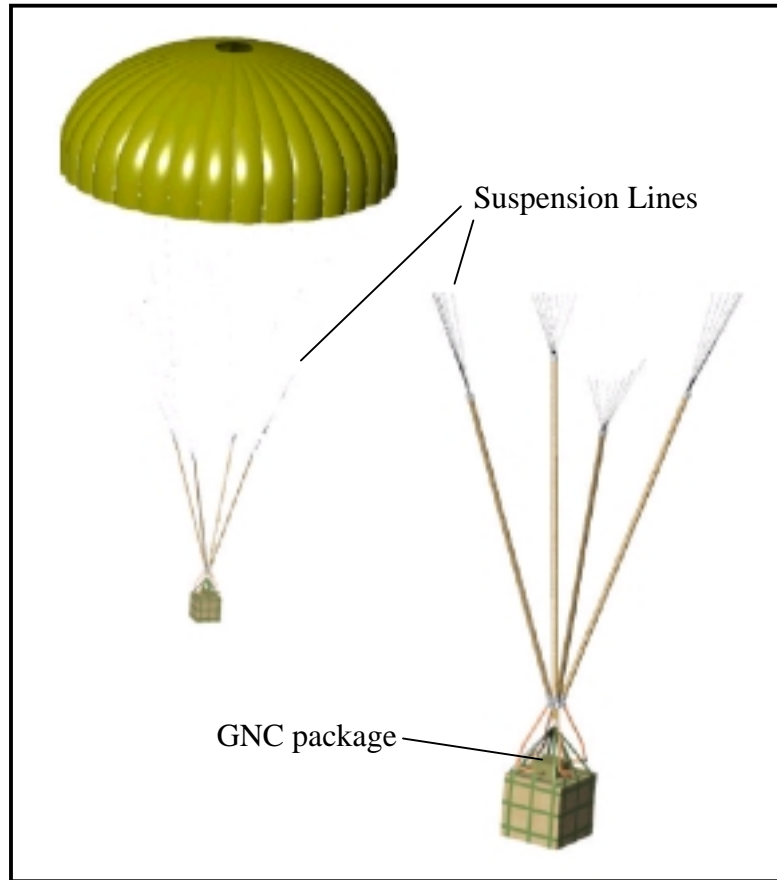
Figure 1. Affordable Guided Airdrop System[1]

B. PARACHUTE

The C-9 parachute was selected for this feasibility demonstration due to its availability and representation of the larger cargo-type parachutes (G-11 and G-12) on which this system will utlimately be used. Although the C-9 was initially designed as an ejection seat parachute, it is a standard flat circular parachute as are the larger G-11 and

---

[1] Couresty of Vertigo, Incorporated, Lake Elsinore, California.

G-12 cargo parachutes. A flat circular parachute is one that when laid out on the ground forms a circle.

Figure 2.   C-9 Parachute

The reference diameters of these chutes are a) 28 feet (C-9), b) 64 feet (G-12), and c) 100 feet (G-11). The reference area of the C-9 parachute is taken to be the total surface area of the canopy (a circle of 28 foot diameter) and is 615.8 square feet. The C-9 is static-line deployed and utilizes 28 suspension lines connecting to four risers.

A cargo box was suspended from the system and housed the remote cotrol system, control actuators, and instrumentation system.

C.   ACTUATORS

Vertigo, Incorporated developed Pneumatic Muscle Actuators[3] (PMAs) to effect the control inputs for this system. The PMAs are braided fiber tubes with neoprene inner sleeves that can be pressurized. Uninflated PMAs as installed on a scaled system are shown in Figure 3. Upon pressurization, the PMAs contract in length and expand in diameter.

4 PMAs are used in
the AGAS system

Figure 3.　Pneumatic Muscle Actuators (PMAs)

With four independently controlled actuators, two of which can be activated simultaneously, eight different control inputs can be affected.　For this demonstration, a throw of approximately 3 feet was selected [measured to be 3.25 feet during ground testing].　When depressurized, the PMAs are completely flexible allowing for efficient packing of the actuators with the parachute.

Figure 4.　Packing the Parachute and Actuators

The concept employed for the AGAS is to fully pressurize all actuators upon successful deployment of the parachute. To affect control of the system, one or two actuators are depressurized. This action "deforms" the parachute creating drive in the opposite direction of the control action. Figure 5 illustrates this action while the Figure 6 illustrates the parachute deformation upon control actuation.
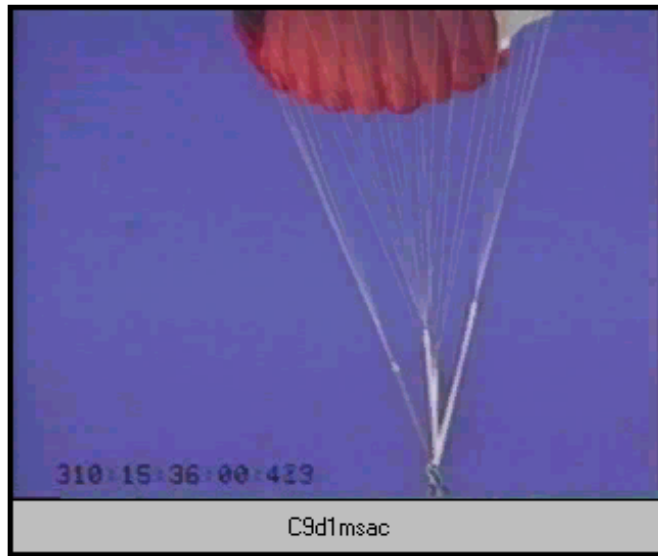

Figure 5.   PMA Actuation (video clip)

Figure 6.   Parachute Response to Control Input (video clip)

D.   MASS AND CENTER OF GRAVITY

The weight of the major system components was determined through direct measurement or calculation using known material weights (e.g. parachute canopy fabric weight of 1.1 ounces per yard). The major system component weights are summarized in Table 1.

The theoretical center of gravity of the system was found to be 11.4 feet from the center of the payload for a standard atmosphere. This calculation includes the mass of the trapped air in the canopy and as such is dependent on the air density. The relationship of center of gravity to density is as follows:

(1) $$l_{cg} = [l_p(\rho V g + W_p) + l_a W_a + l_l W_l + l_c W_c]/W_{system}$$

Substituting known parameters equation 1 reduces to:

$$l_{cg} = 4323\rho + 0.5 \text{ feet and } P_o = \begin{bmatrix} 0 \\ 0 \\ l_{cg} \end{bmatrix} = \begin{bmatrix} 0 \\ 0 \\ 4323\rho + .5 \end{bmatrix}$$

Component	Weight (pounds) sea level - standard atmosphere
Parachute	7.5
Suspension Lines	4.5
Actuators (total for four)	13.3
Payload cargo box instrumentation actuator valves/nitrogen tanks	320.7
Total System	*346.0*

Table 1.   System Weight

E.   MOMENTS OF INERTIA

The moments of inertia of the parachute (including trapped air mass), payload, suspension lines, and actuators were determined as shown below. A summary of these

values is shown in Table 2. Due to symmetry of the parachute and payload system, all

cross products of inertia where assumed to be zero.

Component	Moment of Inertia (slugs·ft²) sea level - standard atmosphere		
	I_{XX}	I_{YY}	I_{ZZ}
Parachute	1865.9	1865.9	211.3
Suspension Lines	neglected		
Actuators (total for four)	neglected		
Payload	1328.3	1328.3	39.9
cargo box			
instrumentation			
actuator valves/nitrogen tanks			
Total System	*3194.2*	*3194.2*	*251.2*

Table 2.   Moments of Inertia

1.   Parachute

When inflated, a flat circular parachute approximates a hemisphere with a radius (r).

The moments of inertia can be found as follows:

(2)
$$I_{XX} = I_{YY} = I_{ZZ} = \frac{2}{3}mr^2.$$

These values then must be translated to the principal axis located at the center of

gravity at the system. The parallel axis theorem[4] is applied as follows:

(3)
$$I_{XX'} = I_{YY'} = I_{XX} + md_x^2 \ and \ I_{ZZ'} = I_{ZZ}.$$

(4)
$$I_{XX'} = I_{YY'} = \frac{2}{3}mr^2 + md_x^2 \ where: \ d_x = d_p - l_{cg}.$$

The moment of inertia, like that of the center of gravity, varies with air density as the

trapped air mass is a significant contributer to this term. Substituting $m = m_p + \rho Vg$ and

all known parameters:

$$I_{XX'} = I_{YY'} = 734436\rho + 1449.0$$

9

$$I_{ZZ} = 83152\rho + 53.5$$

2. Payload

The cargo box dimensions were 2 feet by 2 feet by 2 feet. It is assumed that the center of gravity of this box was located at the center of the box.

The moments of inertia can be found as follows:

(5)
$$I_{XX} = I_{YY} = I_{ZZ} = \frac{1}{2}m(a^2 + l^2); \; where \; a = l.$$

Again applying the parallel axis theorem, the moments of inertia about the principal axis were found. The parallel axis theorem is applied as follows:

(6)
$$I_{XX'} = I_{YY'} = I_{XX} + md_x^2 \; and \; I_{ZZ'} = I_{ZZ}.$$

3. Actuators and Suspension Lines

The actuators and suspension lines were treated as slender rods with the body axis located at the end of the rod. The moments of inertia were found as follows:

(7)
$$I_{XX} = I_{YY} = \frac{1}{3}ml^2 \; and \; I_{ZZ} = 0.$$

These values for this system were found to be extremely small as compared to the values for the parachute and payload and therefore were considered negligible.

III. CONTROL SYSTEM

For an airdrop mission, the aircrew will determine the Computed Air Release Point (CARP) based on the best wind estimate available at that time. The aircraft will then be navigated to that point for air delivery of the materiel. Should the wind estimate and calculation of the predicted release point be perfect and the aircrew gets the aircraft to the precise release point, then the parachute would fly precisely to the target without control inputs. However, wind estimation is far from a precise science. The calculation of the CARP relies on less than perfect estimates of parachute aerodynamics and the flight crews cannot possible precisely hit the predicted release point for each airdrop mission. Therefore, the AGAS control system design must help overcome these potential errors.

Considering the relatively low glide ratio demonstrated in flight test (approximately 0.4-0.5) with a decent rate of approximately 25 feet per second, the AGAS could only overcome an twelve foot per second (approximately 7 knots) wind. It is therefore imperative to implement the system to overcome poor estimates in the wind and not try to steer the system against the entire wind. In other words, the drive of the system is insufficient to attempt to fly straight to the target but is sufficient to overcome up to an twelve foot per second error in the wind estimate. For this reason, a trajectory control approach was selected.

A pre-planned trajectory, based on the best wind estimate available, must be determined and provided to the guidance computer. The GPS navigation system will provide continuous position of the system. The guidance computer will compare the actual horizontal position, at the system's current altitude, to the planned trajectory at that altitude. This represents the position error (P_e) at the current time.

A tolerance cone is established about the planned trajectory (Figure 7) starting at 600 feet at the beginning of the trajectory and gradually decreasing to 60 feet at ground level. Should the position error be outside this tolerance, a control is activated to slip the system back to the planned trajectory. When the system is within 30 feet of the planned trajectory the control is disabled and the parachute drifts with the wind. Thirty feet was selected to encompass approximately 1-sigma of the GPS errors (Selective Availability off).
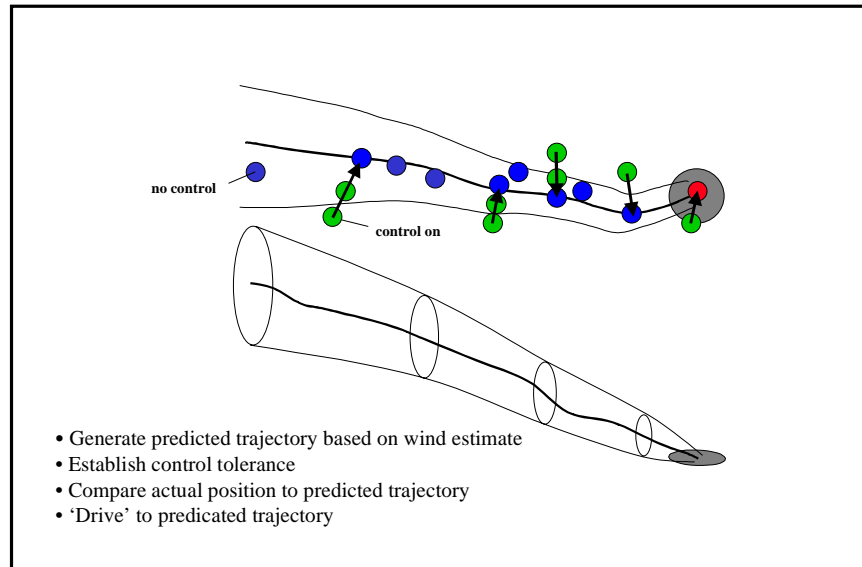

Figure 7.   Control Concept (double click to see animation)

As outlined above, the control system relies on the current horizontal position error to determine if control input is required. This position error (P_e) is determined in inertial space and is then rotated to the body axis using an euler angle rotation with heading only. The resultant body-axis error (P_b) is then used to identify which control input must be activated as shown in Equation 8. Two components are returned, a + or - for the x-axis and a + or - for the y-axis. It was assumed for this simulation that a +x would activate control A, a -x activates control C, a +y activates control B, while a -y activates control

D. The actual rigging of the operational system must align these control actuators to the compass reference line to ensure proper control. Control A is assumed to be aligned with the compass zero reference line.

(8)
$$input = sign\left(\frac{P_b}{\|P_b\|}\right);$$

The magnitude of this calculation is used to determine if the selected control input will be activated. If the magnitude is greater than 0.3, then that control is activated. This will allow the activation of a single control input or two simultaneous control inputs. Preventing activation of control when this value to less than 0.3 will ensure that unnecessary control inputs are not activated when the predominate error is in a single direction. Figure 8 illustrates the region of active control.
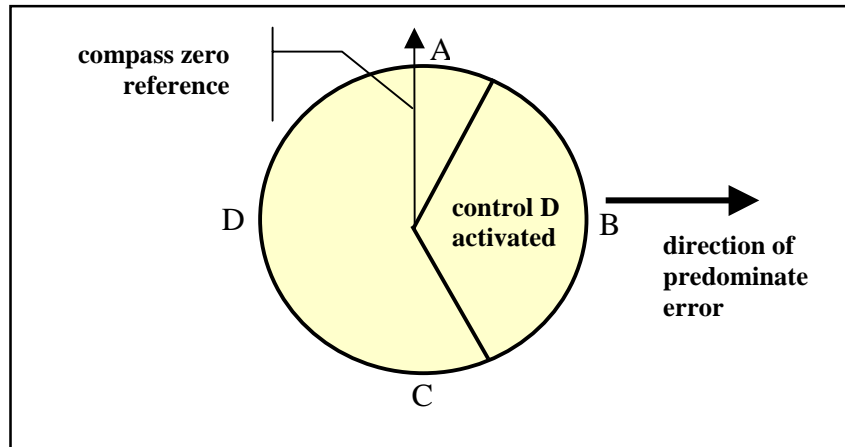

Figure 8.   Control Activation

IV.   TESTING

The objectives of the test program were to investigate the apparent mass effects on flat circular parachutes and to obtain sufficient data to assess the feasibility of the AGAS concept. To meet these objectives, ground testing of the C-9 parachute and flight testing of the prototype AGAS, using remotely controlled activation of the actuators was conducted.

A.   INVESTIGATION OF APPARENT MASS EFFECTS

To illustrate the effects of apparent mass on the dynamics of a parachute, a test program was established to collect the forces along the z-axis of the parachute during acceleration. The concept defined by Vertigo, Incorporated[5] to evaluate the apparent mass terms was implemented. The C-9 parachute was attached, to a tower installed on the vehicle, with two attaching risers and towed behind a ground vehicle (Figure 9).

Figure 9.   Tow Test

The vehicle first accelerated to a speed of approximately 10 feet per second, after a brief period of constant velocity, the vehicle accelerated at a near constant acceleration. Figure 10 shows a typical velocity profile for these tests.
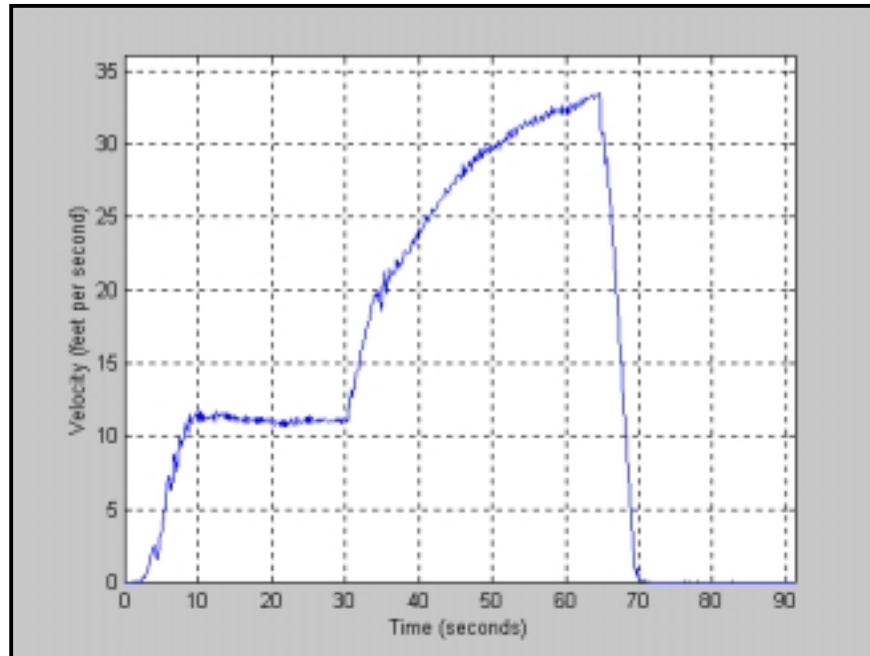

Figure 10. Tow Test Velocity Profile

The forces in the attaching risers were measured with strain gauges. In addition, a "box" was constructed on top of the tower to measure the vertical and lateral forces on the riser attachment points. By measuring these forces, an estimate of the parachute angle of incidence could be derived. Figure 11 illustrates the instrumentation configuration at one riser attachment point. The velocity was measured with differential GPS and an anemometer.

To estimate the actual apparent mass parameters, motion of the parachute would be ideally fixed in one direction. In the Vertigo test, the BZA parachute was very stable.

Therefore, the assumption of motion in only one axis is very reasonable. With the C-9 parachute, significant oscillations were observed.
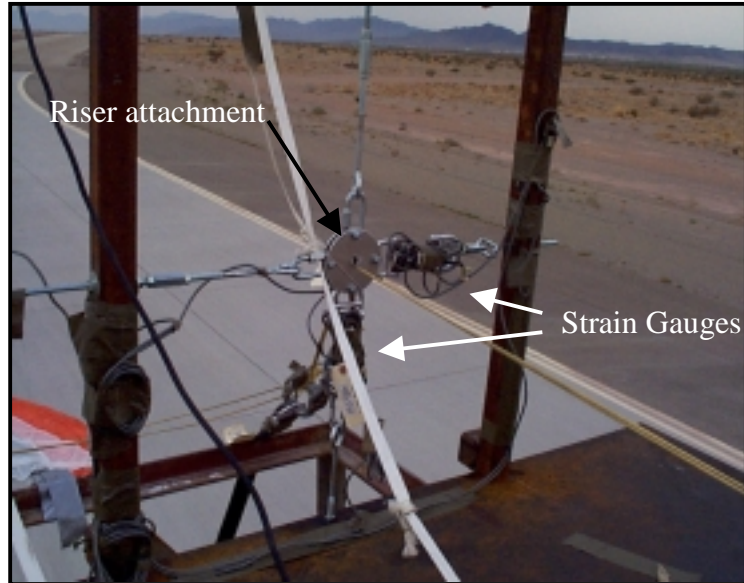

Figure 11. Instrumentation Configuration: Riser Attachment

A plot of the calculated incidence angle (φ) demonstrates the oscillatory nature of this parachute. Therefore, estimation of the apparent mass coefficients using these techniques was not possible.
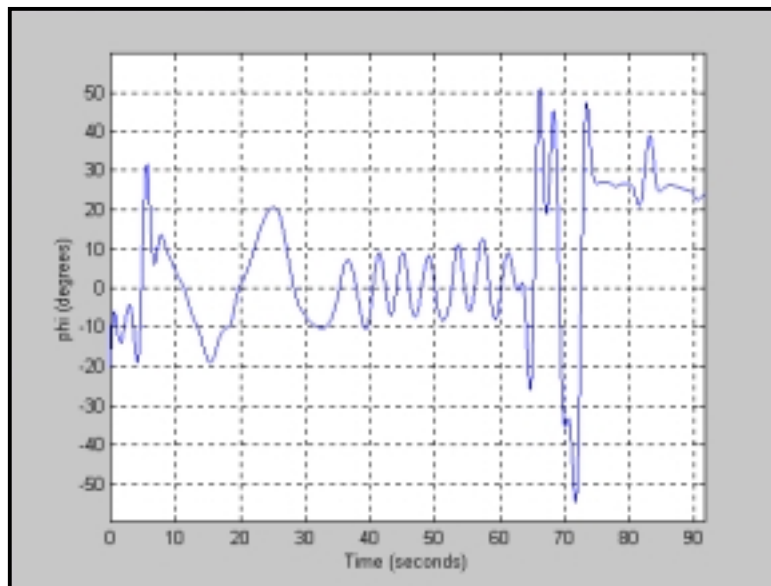

Figure 12. Incidence Angle (φ)

Even though precise apparent mass coefficients cannot be found, insight to the apparent mass contributions can be gained by analyzing these data. Figure 13 demonstrates the influence of apparent mass on parachute dynamics. The total force along the parachutes z-axis, as measured in the risers, is plotted along with the steady state drag calculations as found by:

(9) $$D_{ss} = \frac{1}{2}\rho V^2 \cdot S_o \cdot C_D ;\ \textit{where } S_o \textit{ is the reference area of the parachute and}$$

C_D is the steady-state drag
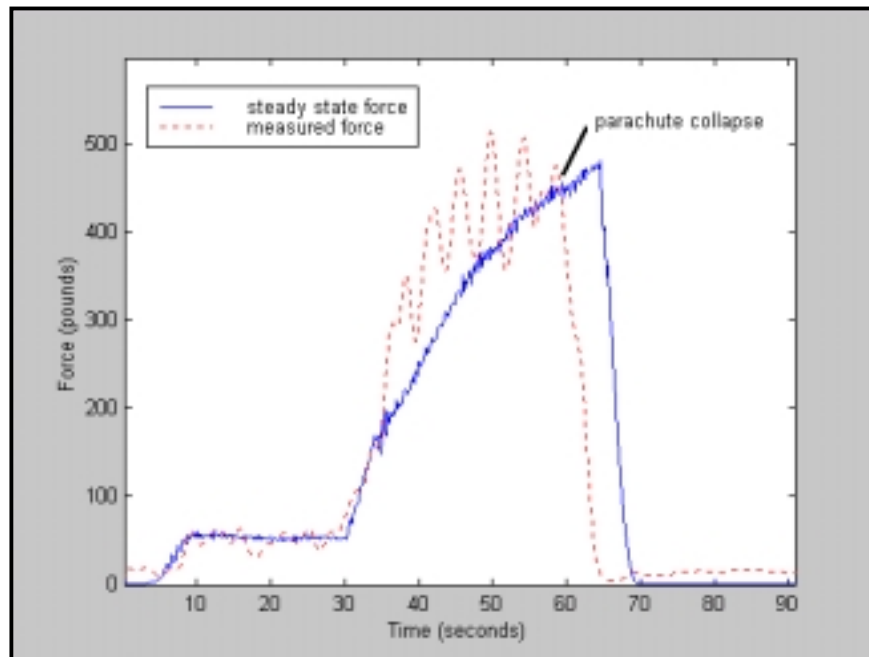

coefficient (0.68).

Figure 13. Apparent Mass Effects on Parachute Dynamics

The figure shows increased measured force above the predicted steady-state drag along the parachute when the parachute is accelerating. Note during the first accelerations that the measured force did not rise above the steady state drag estimate. This is likely due to the parachute inflation and the greatly changing angle of incidence during this inflation. Concentrating on the area where the parachute has settled into pure

oscillations, the apparent mass effects can be observed. Figure 14 presents an excerpt of data for this time:
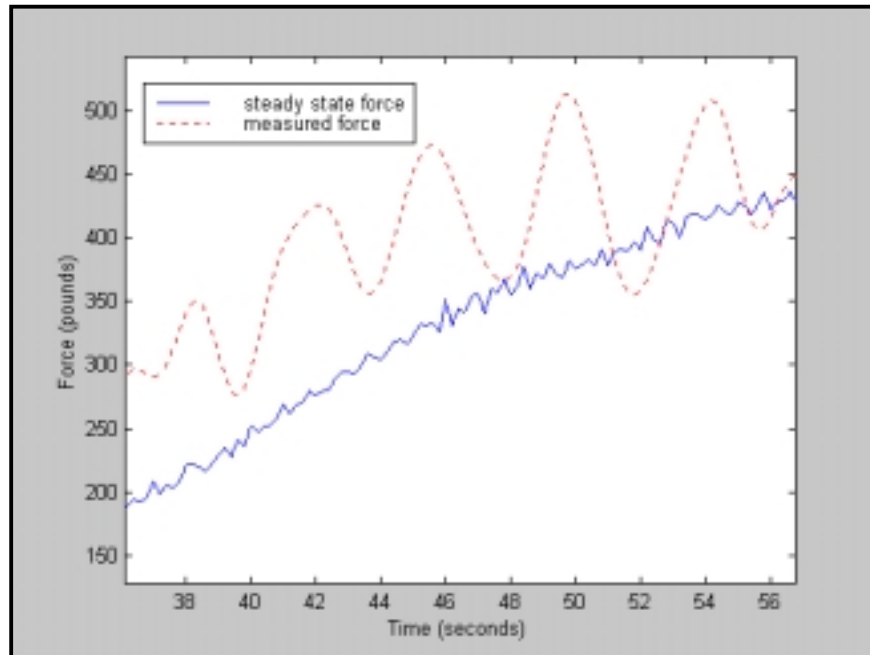

Figure 14. Apparent Mass Effects

These data demonstrate the apparent mass effects must be considered in flight dynamic modeling. Even with the relatively small accelerations experienced here, the effect is very large and varies greatly with acceleration of the parachute (as observed with the oscillating parachute).

B. FLIGHT TESTING

The flight test effort focused on the collection of flight dynamic data to support modeling of the AGAS concept. The flight test effort was conducted with four actuators in-line with a C-9 parachute and one-half scale container delivery system. The actuators were activated using a manual radio control system. Flight dynamic data was obtained including the position, velocity, acceleration, attitude, and attitude rates of the system. It

was necessary to correlate these data with control inputs. Therefore, the state of control activation was monitored. Parachute performance is significantly influenced by the winds. It was critical to this effort to measure the winds as precisely as possible.

C. INSTRUMENTATION

Ideally, both the parachute and payload would have been instrumented to collect all necessary data. However, the state-of-the-art in instrumentation is not yet sufficient to adequately instrument the parachute itself. As a result, only the payload could be instrumented. A custom instrumentation system was developed and included a differential GPS system for precise position and velocity, 3-axis accelerometers for acceleration, and a Attitude Heading and Reference System (AHRS) for 3-axis attitudes and attitude rates. Pressure transducers were put in line with the pneumatic actuators to monitor their action. Figure 15 illustrates the instrumentation design. A summary of the major instrumentation components is provided in Appendix E.
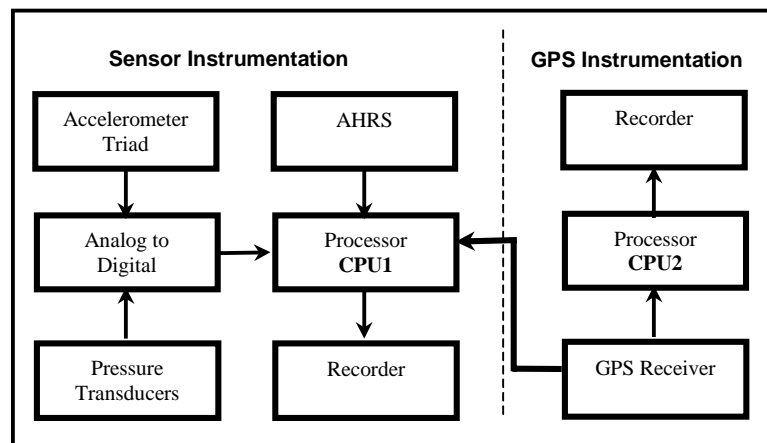

Figure 15. Instrumentation Block Diagram

The critical part of this design is the time synchronization of data from all sources. To achieve this, the IRIG time generator was synchronized with GPS time using the

Havequick Time Interface and the 1-Pulse Per Second time sync. The AHRS data is provided on its interface approximately 71 times per second. This is the fastest rate for all the sensors. Therefore, these data were used as the key for capturing data from all sensors. When an AHRS message was first detected by CPU1, the first record was time-tagged and the entire message was sent to the recorder. At that time, the Analog-Digital (A-D) converter was polled for its data. The first record from the A-D converter was time-tagged and the message sent to the data recorder. The GPS data from the differential receiver was independently captured (with an embedded time-tagging using GPS time) and recorded on a separate PC-Card. The synchronization of the data was validated in two ways. First, it was desired to have a discrete event that would effect all data sensors. The obvious event was ground impact, which resulted in immediate changes in the data from each sensor. This discrete event showed the data from the independent sensors was time synchronized to less than 200 milliseconds (the rate of GPS data). Next, the acceleration data was integrated to estimate velocity. This estimated velocity was then compared to the GPS velocity (after rotation from the body to inertial reference frame using the AHRS attitude data). These results also showed the data was time-tagged to within 200 milliseconds.

D.   WIND ESTIMATION

Two methods of wind estimation are presented. The first includes the accepted standard of the Radiosonde Wind Measuring System (RAWIN) system used throughout the test community. A RAWIN balloon was launched at approximately one-hour intervals near the release time in the vicinity of the Drop Zone. This system provides a direct measurement of the winds as a function of altitude. Although an accepted

standard, the RAWIN system has limitations in airdrop operations. The largest problem is that real-time winds are not available. The balloon must be launched and data processed resulting in approximately a one-hour delay. Figure 16 illustrates the magnitude of wind changes over time. Data from three RAWIN launches are presented as a function of altitude. It is clear that, as the parachute gets close to the ground, the wind changes can be significant.
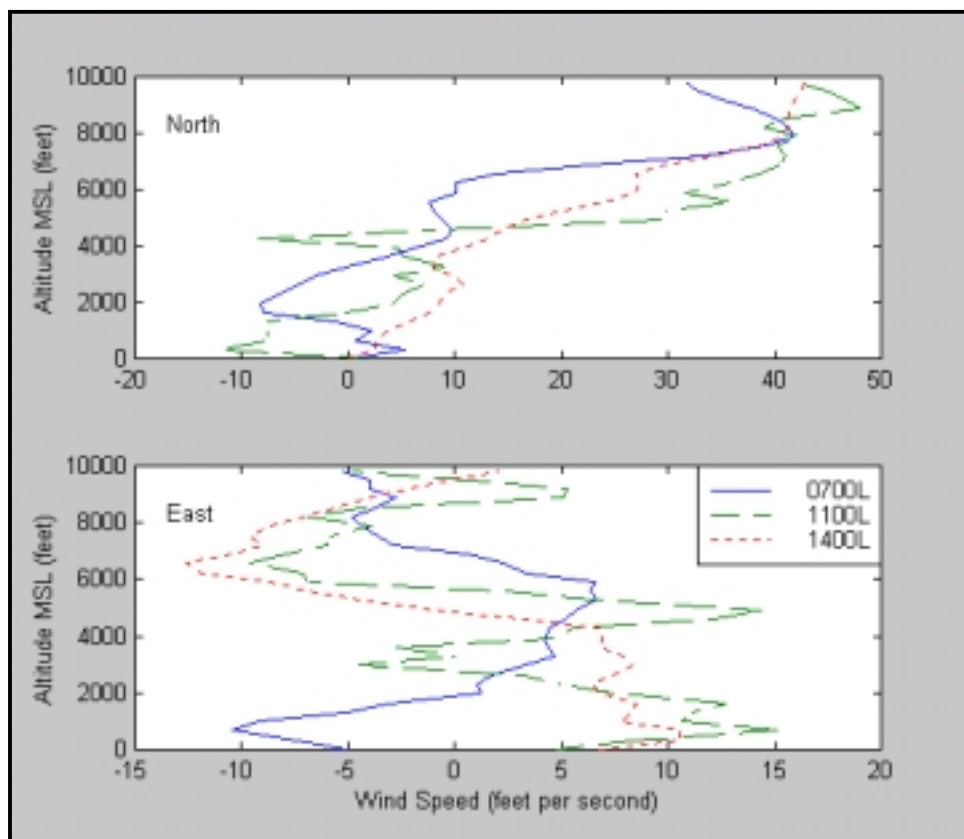

Figure 16. Wind Changes Over Time

A second method of deploying a "calibration system" just prior to release of the test payload was implemented. A tri-lobe parachute was used with a reference drag area (C_DS) of 90.88. Oscillations of this parachute were observed to be very small. The system was weighted at 58 pounds to provide approximately the same descent rate as the

C-9 system. The calibration system was instrumented with differential GPS on the payload. Initially, the wind estimate was simply taken as the ground velocity as measured by the GPS. This approach effectively considers the calibration system massless and therefore does not account for changes in momentum.

To validate the ability to simply use the measured ground track velocity as the wind estimate, a model of the calibration parachute system was developed. A point-mass system was assumed with the only forces on the system being drag and weight. The applicable equations of motion are:

(10) $$X = (m + \alpha_{11})\dot{u} = -D\cos\gamma\cos\psi$$

(11) $$Y = (m + \alpha_{22})\dot{v} = -D\cos\gamma\sin\psi$$

(12) $$Z = (m + \alpha_{33})\dot{w} = -D\sin\gamma + W$$

where: W is the calibration system weight, D is drag ($D = qC_D S$), γ and ψ are the flight path angle and yaw angle respectfully.

The reference angles are:

(13) $$\sin\gamma = \frac{w}{V_T}; \quad \cos\gamma = \frac{\sqrt{V_T^2 - w^2}}{V_T}; \quad \sin\psi = \frac{v}{\sqrt{V_T^2 - w^2}}; \quad \cos\psi = \frac{u}{\sqrt{V_T^2 - w^2}}$$

Substituting, rearranging terms, and putting in state space form:

(14) $$\begin{bmatrix} \dot{u} \\ \dot{v} \\ \dot{w} \end{bmatrix} = \begin{bmatrix} m + \alpha_{11} & 0 & 0 \\ 0 & m + \alpha_{22} & 0 \\ 0 & 0 & m + \alpha_{33} \end{bmatrix}^{-1} \left\{ \frac{-qC_D S}{V_T} \begin{bmatrix} u \\ v \\ w \end{bmatrix} + \begin{bmatrix} 0 \\ 0 \\ W \end{bmatrix} \right\}$$

where: α_{xx} are the apparent mass terms, here assumed to be constant

Noting that:

$V_G = V_A + V_W$; where V_G = ground velocity, V_A=velocity relative to the local air mass (airspeed), V_W=wind velocity. Assumes no rotation between the fixed earth reference and the system's body axis.

(15)
$$\dot{V}_G = \dot{V}_A + \dot{V}_W$$

Equation 14 presents the equation for $\dot{V}_A$. The GPS instrumentation measures ground speed, applying 15 to 14:

(16)
$$\dot{V}_G = \begin{bmatrix} \dot{u} \\ \dot{v} \\ \dot{w} \end{bmatrix}_G = \begin{bmatrix} m+\alpha_{11} & 0 & 0 \\ 0 & m+\alpha_{22} & 0 \\ 0 & 0 & m+\alpha_{33} \end{bmatrix}^{-1} \left\{ \frac{-qC_D S}{V_T} \begin{bmatrix} u \\ v \\ w \end{bmatrix} + \begin{bmatrix} 0 \\ 0 \\ W \end{bmatrix} \right\} + \dot{V}_W$$

Equation 16 can be solved numerically to estimate the system response to the estimated winds and compared to the measured velocity of the system. Using the measured ground track velocity as the initial wind estimate, the modeled ground track was determined. The difference between this modeled ground track and the actual measured ground track reflects the errors in the wind estimate. The magnitude of these errors indicates the significance of accounting for momentum changes caused by changes in the wind. A Simulink® model was implemented (Figure 17).
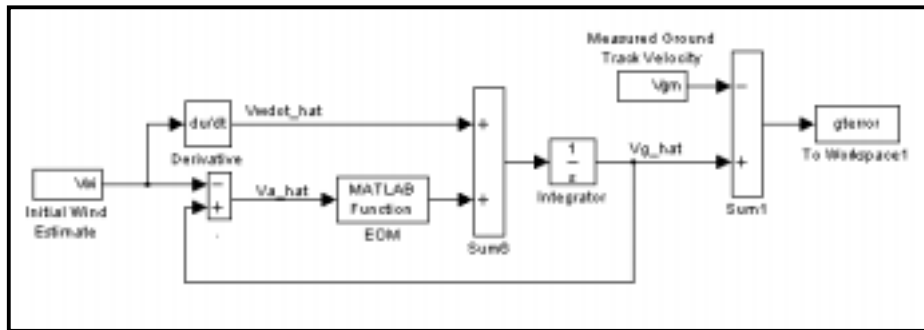

Figure 17. Simulink® Realization for Wind Estimation

® Registered trademark of Mathworks, Inc., Natick, MA

23

Figures 18 presents the results of this validation. Use of the measured ground track velocity as the wind estimate, resulted in errors less than 0.3 feet per second.
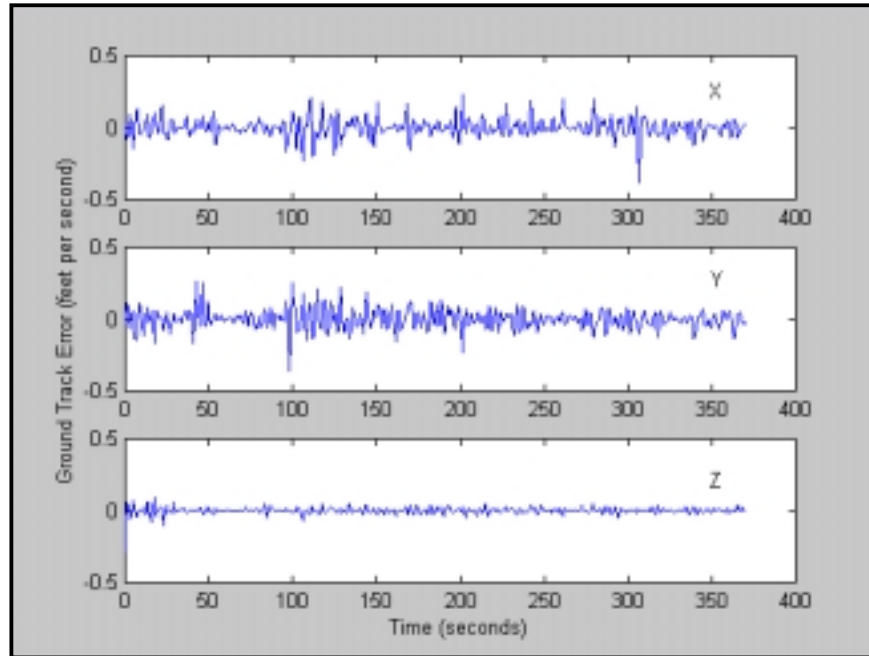

Figure 18. Wind Estimation Results

To further assess this technique, the equations for wind estimation utilized with hurricane dropsondes[6] was applied. In this application, the 3-dimensional velocity of a dropsonde is determined. The horizonal velocity components of the air mass are then found as follows:

(17) $$x_W \approx \dot{x} - \frac{\ddot{x}\dot{z}}{g} \ and \ y_W \approx \dot{y} - \frac{\ddot{y}\dot{z}}{g}; \ where$$

To apply equation 17, a Simulink® model was implemented (Figure 19). The correction that would be applied to the horizontal velocity is presented in Figure 20. These data show that the corrected wind estimate, using the hurricane approach, differs from the measured ground track by less than 0.3 feet per second. More errors are seen

close to ground impact where additional shears are present. This is not of consequence

for this study as the flight dynamic data of interest is at much higher altitude.
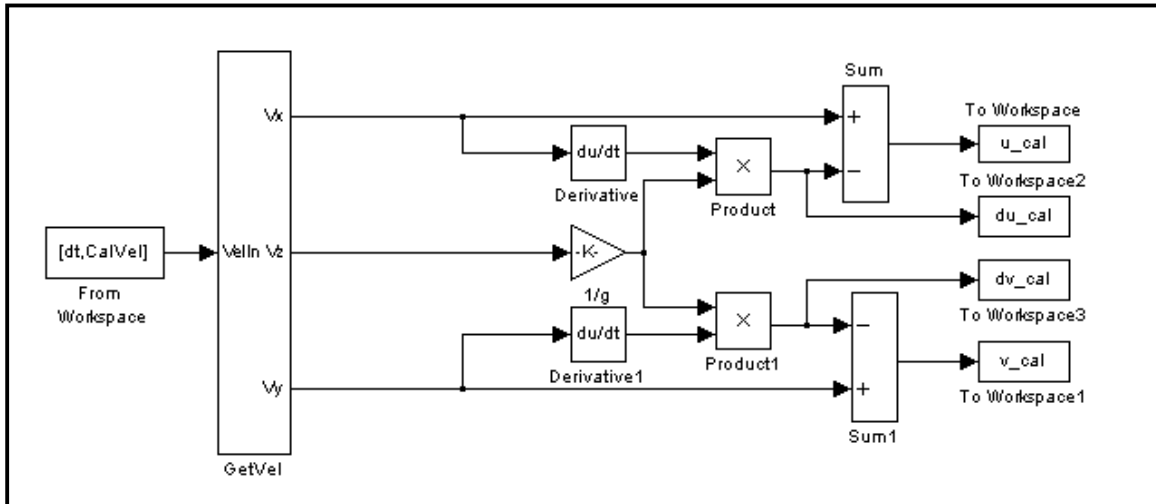

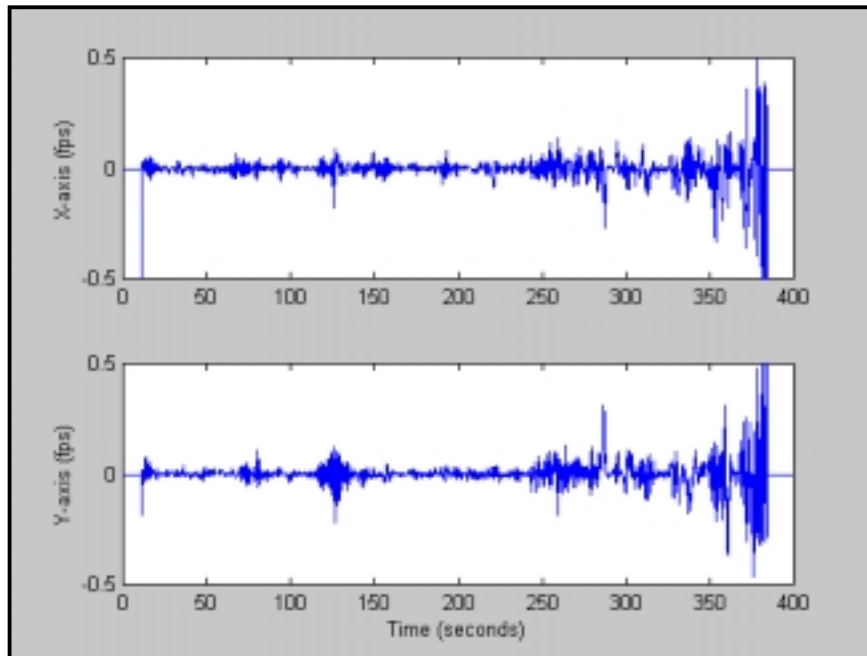Figure 19.   Hurricane Wind Estimation Implementation

Figure 20. Hurricane Wind Estimation Results

These results indicate that the momentum effects can be ignored for wind estimation

for the selected parachute system. Figure 21 illustrates the comparison of the wind

estimate to the winds measured by the RAWIN. Recall that the RAWIN balloon was launched only every hour. The closest RAWIN data was used for this comparison.
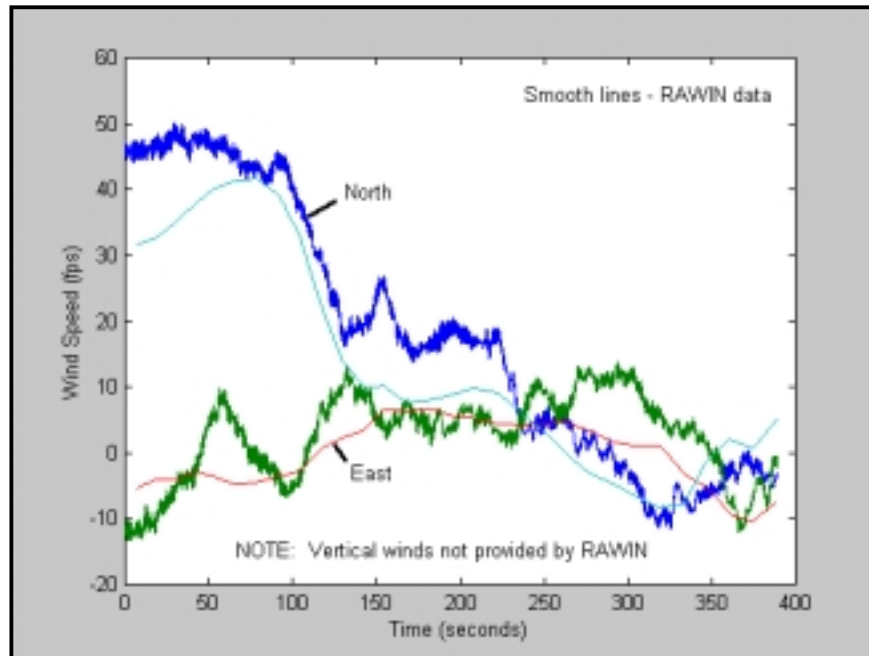

Figure 21. Wind Estimation Compared to RAWIN

These results demonstrate this technique will provide significantly better estimates of winds than using the RAWIN system. By weighting the calibration system with to match the descent rate of the test item, the two parachutes will be subjected to the same (as close as possible) atmospheric conditions. Using the measured GPS ground track velocities is an adequate approximation for wind estimation. Other techniques such as that presented above may provide some refinement on the wind estimates but the difference is likely to be insignificant for most testing. The key to application of this technique is the use of a very stable parachute due to the reductions in apparent mass effects resulting from oscillations.

E.   DATA REDUCTION

Data from all sources were time correlated using the AHRS time tag. As this data was recorded at the fastest rate, all other data parameters were correlated with this time field. A linear interpolation was used to estimate the acceleration, actuator movement, and trajectory of the AGAS system at the time of the AHRS measurement. The data recorded on the calibration parachute (differential GPS only) was correlated to the system data again using linear interpolation. Instead of time correlating, the calibration data was correlated to the AGAS trajectory data with the AGAS altitude. As previously discussed, the velocity data from the calibration parachute was taken as the wind without any processing (excluding the vertical). For the vertical winds, the mean and density effects were removed from the calibration parachute vertical velocity.

The performance of the C-9 parachute is characterized by significant oscillations in both pitch and roll. The larger G-12, to be used in the operational configuration, is not expected to oscillate as severely as this parachute.

Figure 22. Parachute Oscillations (video clip)

27

The system instrumentation was all located in the payload and therefore measured the movement of the payload induced from the oscillations. The velocity data best demonstrates this character (Figure 23).
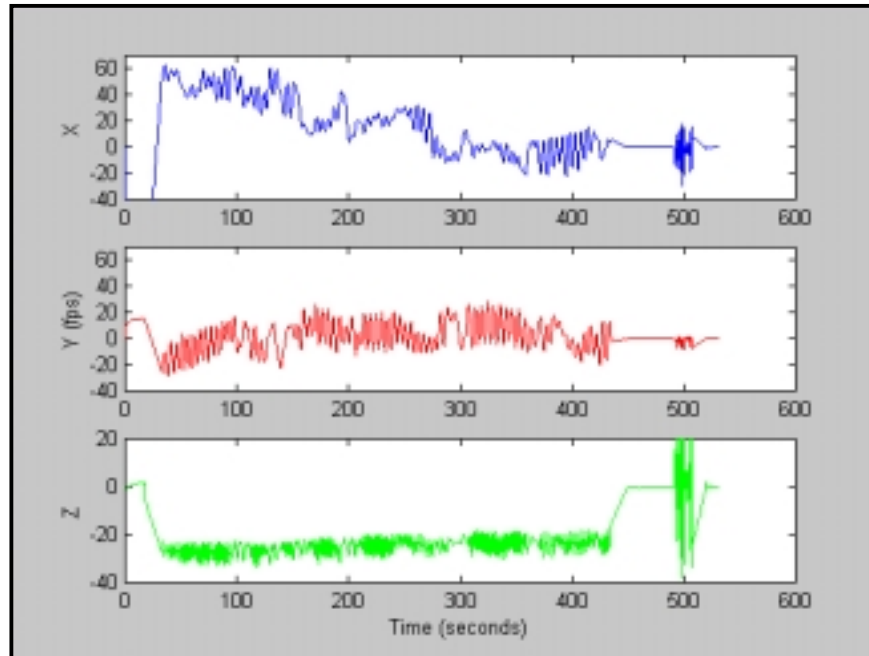

Figure 23. Data Characteristics Due to Oscillations

To better represent the operational system during this feasibility test, attempts were made to modify the C-9 parachute to minimize the oscillations by cutting large symmetrical slots in the canopy. This modification proved very stable during tow testing as well as the initial test drop. The system was then dropped with one riser extended representing a single control input. The objective of this drop was to qualitatively assess the amount of drive that could be obtained with this modified parachute. There was insufficient indication that this modification allowed enough drive for the guided system. Had the results been favorable, additional instrumented drops with the actuator/control system would have been accomplished.

Since the trials with the modified parachute did not present the desired results, the oscillation in the data need to be dealt with prior to parameter estimation. These data must be corrected to the location of the system's center-of-gravity.

Starting with the position corrections:

(18) $$P_{CG} = P_L + {}^U_B R L; \quad \text{where } P_L \text{ is the measured position of the payload and } L \text{ is}$$

the lever-arm from the location of the instrumentation to the center of gravity in body-axis coordinates {B}.

The velocity correction is then given by:

(19) $$V_{CG} = \dot{P}_{CG} = \dot{P}_L + {}^U_B \dot{R} L + {}^U_B R \frac{d}{dt} L$$

Recalling:

(20) $${}^U_B \dot{R} L = {}^U_B R S(\omega) L = {}^U_B R (\omega x L)$$

Substituting (20) into (19):

(21) $$V_{CG} = \dot{P}_L + {}^U_B R (\omega x L) + {}^U_B R \frac{d}{dt} L$$

For rigid bodies, L is assumed constant and therefore $\frac{d}{dt} L = 0$.

Applying this condition to a parachute did not yield adequate results, as the oscillations were still apparent in the velocity data. It is presumed that in an oscillating parachute, the forces on the parachute are changing due to the linear acceleration induced by the oscillations (apparent mass effects) while the forces on the payload are not varying. With this imbalance of forces in the parachute and payload, an effective change in center-of-gravity of the system results.

To illustrate this situation, the lever-arm correction is determined:

Rearranging (21)

(22) $$L = {}_U^B R (P_{CG} - P_L)$$

P_L is measured. P_{CG} is estimated using the measured velocity at the payload (V_L). A low-pass filter is applied to V_L to remove the effect of the oscillations. Using this filtered velocity (V_{LF}) and removing the wind velocity (V_W), an estimate of the velocity at the center-of-gravity is obtained (V_{CG}).

(23) $$V_{CG} \approx V_{LF} - V_W$$

This velocity is then integrated from the parachute release point. The estimated location of the center-of-gravity was then determined using Equation 22. Figure 24 presents these results.
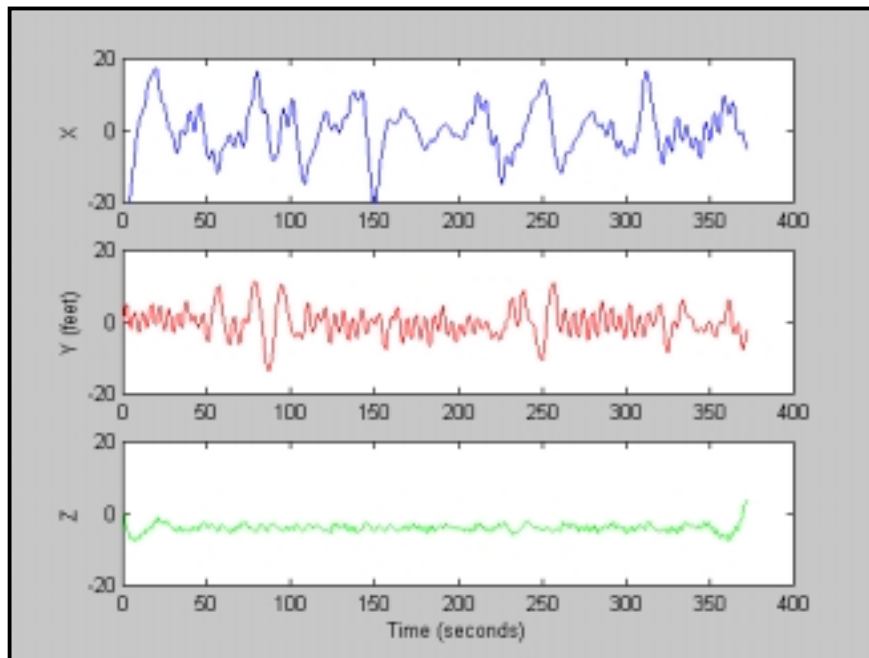

Figure 24. Movement of Lever Arm Correction

The mean lever arm corrections are: L_x=0.0, L_y=-0.1, and L_z=-3.94 feet. Yavus and Cockrell demonstrated that acceleration of the air mass and angle of attack of the parachute significantly affects the apparent mass coefficients[7]. Attempts were made to correlate these data to linear and angular acceleration of the payload. However, no direct correlation could be found. Ideally, acceleration of the parachute should be measured in future work. With the existing instrumentation suite, it appears the flight test data must be filtered to remove the effects of oscillations prior to parameter estimation. Using the data obtained from the uncontrolled test drop (311drop1), a filter was derived using the

MATLAB[®] System Identification Tools. A 5th-order low-pass filter with a cut-off frequency of 0.009 (in fractions of the Nyquist frequency) was selected. Figure 25 compares the measured data to the filtered data for velocity.

Figure 25. Comparison of Measured and Filtered Velocities

[®] Registered trademark of Mathworks, Inc, Natick, MA.